

# Inhibition effect of environmentally benign Karanj (*Pongamia pinnata*) seed extract on corrosion of mild steel in hydrochloric acid solution

Ambrish Singh · Ishtiaque Ahamad · V. K. Singh ·  
Mumtaz Ahamed Quraishi

Received: 15 April 2010 / Revised: 4 August 2010 / Accepted: 6 August 2010 / Published online: 19 August 2010  
© Springer-Verlag 2010

**Abstract** The inhibition of the corrosion of mild steel in hydrochloric acid solution by the seed extract of Karanj (*Pongamia pinnata*) has been studied using weight loss, electrochemical impedance spectroscopy, potentiodynamic polarization, and linear polarization techniques. Inhibition was found to increase with increasing concentration of the extract. The effect of temperature, immersion time, and acid concentration on the corrosion behavior of mild steel in 1 M HCl with addition of extract was also studied. The adsorption of the extract on the mild steel surface obeyed the Langmuir adsorption isotherm. Values of inhibition efficiency calculated from weight loss, potentiodynamic polarization, and electrochemical impedance spectroscopy are in good agreement. Polarization curves showed that Karanj (*P. pinnata*) seed extract behaves as a mixed-type inhibitor in hydrochloric acid. The activation energy as well as other thermodynamic parameters for the inhibition process was calculated. The adsorbed film on mild steel surface containing Karanj (*P. pinnata*) seed extract inhibitor was also measured by Fourier transform infrared spectroscopy. The results obtained showed that the seed extract of Karanj (*P. pinnata*) could serve as an effective inhibitor of the corrosion of mild steel in hydrochloric acid media.

**Keywords** Karanj (*Pongamia pinnata*) · Corrosion inhibition · Mild steel · Electrochemical measurement · FTIR · Hydrochloric acid

A. Singh · V. K. Singh  
Department of Chemistry, Udai Pratap Autonomous College,  
Varanasi 221002, India

I. Ahamad · M. A. Quraishi (✉)  
Department of Applied Chemistry, Institute of Technology,  
Banaras Hindu University,  
Varanasi 221005, India  
e-mail: maquraishi.apc@itbhu.ac.in

## Introduction

Inhibitors are frequently used for controlling corrosion of metals and alloys in acidic media for removing scales and rusts in metal finishing industries, cleaning of boilers, and heat exchangers. Use of inhibitors is one of the most practical methods for protection against corrosion especially in acid solutions to prevent unexpected metal dissolution and acid consumption [1, 2]. The known hazardous effect of most synthetic corrosion inhibitors have motivated scientists to use naturally occurring products as corrosion inhibitors as they are inexpensive, readily available and renewable sources of materials, environmentally friendly, and ecologically acceptable [3, 4].

Up until now, many plant leaf extracts such as *Murraya koenigii*, *Embilica officianilis*, *Terminalia chebula*, *Terminalia belivina*, *Sapindus trifolianus*, *Accacia conicianna*, *Swertia angustifolia*, *Eugenia jambolans*, *Pongamia glabra*, *Annona squamosa*, *Accacia Arabica*, *Occimum viridis*, *Telferia occidentalis*, *Carica papaya*, *Azadirachta indica*, *Vernonia amydalina*, *Nypa fructicans* wurmb, *Ricimus communis* coriander, hibiscus, Eucalyptus, anis, black cumin, and garden cress have been studied for the corrosion inhibition of mild steel in acid media [5–10]. Some of the seeds such as tobacco, castor oil seeds, acacia gum, and lignin along with *Papaia*, *Poinciana pulcherrima*, *Cassia occidentalis*, and *Datura stramonium* have also been used as efficient corrosion inhibitor for steel [11–15]. The anticorrosion activity of onion, garlic, and bitter gourd for mild steel in acid media showed good results studied. Oil extracts of ginger, jojoba, eugenol, acetyl-eugenol, *artemisia* oil, and *Mentha pulegium* are used for corrosion inhibition of steel in acid media [16, 17]. Saps of certain plants are very useful corrosion inhibitors. *Calotropis procera*, *Azydracta indica*, and *Auforpio turkiale* saps are

useful as acid corrosion inhibitors. Quinine has been studied for its anticorrosive effect of carbon steel in 1 M HCl. The inhibition effect of *Zenthoxylum alatum* extract on the corrosion of mild steel in aqueous orthophosphonic acid was investigated [18–20].

In continuation of our work on development of green corrosion inhibitors [21, 22], the present study investigates the inhibiting effect of seed extract of Karanj (*Pongamia pinnata*), which is commonly known as Karanj in India. Inhibition effect of Karanj (*P. pinnata*) on the corrosion of mild steel in 1 M HCl solution by weight loss, potentiodynamic polarization, and electrochemical impedance spectroscopy (EIS) methods. Meanwhile, the steel surface was examined by Fourier transform infrared (FTIR) spectroscopy.

## Experimental

### Preparation of Karanj (*P. pinnata*) seed extract

Karanj (*P. pinnata*) seed was dried and ground to powder form. Dried (5 g) powder was soaked in double distilled water (500 mL) and refluxed for 5 h. The aqueous solution was filtered and concentrated to 100 mL. This extract was used to study the corrosion inhibition properties. Corrosion tests were performed on a mild steel of the following percentage composition (wt.%): Fe 99.30%, C 0.076%, Si 0.026%, Mn 0.192%, P 0.012%, Cr 0.050%, Ni 0.050%, Al 0.023%, and Cu 0.135%, which were abraded successively with fine-grade emery papers from 600 to 1,200 grade. The specimens were washed thoroughly with double distilled water and finally degreased with acetone and dried at room temperature. The aggressive solution 1 M HCl was prepared by dilution of analytical grade HCl (37%) with double distilled water, and all experiments were carried out in unstirred solutions.

### Weight loss method

Weight loss measurements were performed on the mild steel samples with a rectangular form of size  $2.5 \times 2.0 \times 0.025$  cm in 1 M HCl solution with and without addition of different concentrations of seed's extract. Every sample was weighed by an electronic balance and then placed in the acid solution (100 mL). The duration of the immersion was 3 h at the temperature range from 308 to 338 K. After immersion, the surface of the specimen was cleaned by double distilled water followed rinsing with acetone, and the sample was weighed again in order to calculate inhibition efficiency ( $\eta$  %) the corrosion rate ( $C_R$ ). The experiments were done in triplicate, and the average value of the weight loss was noted. For each experiment, a freshly

prepared solution was used, and the solution temperature was thermostatically controlled at a desired value.

The aggressive solutions (1 M HCl) were prepared by dilution of an analytical grade HCl with double distilled water. The surface coverage ( $\theta$ ) and inhibition efficiency ( $\eta$  %) was determined by using following equation:

$$\theta = \frac{w_0 - w_i}{w_0} \quad (1)$$

$$\eta\% = \frac{w_0 - w_i}{w_0} \times 100 \quad (2)$$

Where,  $w_i$  and  $w_0$  are the weight loss values in presence and absence of inhibitor, respectively.

The corrosion rate ( $C_R$ ) of mild steel was calculated using the relation:

$$C_R(\text{mm/year}) = \frac{87.6 \times w}{atD} \quad (3)$$

Where,  $w$  is corrosion weight loss of mild steel (mg),  $a$  the area of the coupon ( $\text{cm}^2$ ),  $t$  is the exposure time (h), and  $D$  the density of mild steel ( $\text{gcm}^{-3}$ ).

### Electrochemical measurements

The electrochemical studies were made using a Gamry three-electrode cell assembly at room temperature. The mild steel of  $1 \text{ cm}^2$  was the working electrode, platinum electrode was used as an auxiliary electrode, and standard calomel electrode was used as reference electrode. The working electrode was abraded with different grades of emery papers, washed with water, and degreased with acetone. All electrochemical measurements were carried out using Gamry Potentiostat/Galvanostat (Model G-300) with EIS software Gamry Instruments Inc., USA. Gamry applications include software DC 105 for corrosion and EIS 300 for EIS measurements and Echem Analyst version 5.50 software packages for data fitting. Prior to the electrochemical measurement, a stabilization period of 30 min was allowed, which was proved to be sufficient to attain a stable value of  $E_{\text{corr}}$ .

The linear polarization study was carried out from cathodic potential of  $-20$  mV versus OCP to an anodic potential of  $+20$  mV versus OCP with a sweep rate  $0.125 \text{ mVs}^{-1}$  to determine the polarization resistance ( $R_p$ ). From the measured polarization resistance value, the inhibition efficiency has been calculated using the relationship:

$$\eta\% = \frac{R'_p - R_p^0}{R'_p} \times 100 \quad (4)$$

Where,  $R_p^0$  and  $R'_p$  are the polarization resistance in absence and in presence of inhibitor, respectively.

Tafel curves were obtained by changing the electrode potential automatically from  $-250$  to  $+250$  mV versus corrosion potential ( $E_{\text{corr}}$ ) at a sweep rate of  $1 \text{ mVs}^{-1}$ . EIS measurements were carried out in a frequency range from  $100 \text{ kHz}$  to  $10 \text{ mHz}$  under potentiodynamic conditions, with amplitude of  $10 \text{ mV}$  peak-to-peak, using AC signal at  $E_{\text{corr}}$ . The linear Tafel segments of anodic and cathodic curves were extrapolated to corrosion potential to obtain corrosion current densities ( $I_{\text{corr}}$ ). The inhibition efficiency was evaluated from the measured  $I_{\text{corr}}$  values using the relationship:

$$\eta\% = \frac{I_{\text{corr}}^0 - I_{\text{corr}}'}{I_{\text{corr}}^0} \times 100 \quad (5)$$

Where,  $I_{\text{corr}}^0$  and  $I_{\text{corr}}'$  are the corrosion current in absence and in presence of inhibitor, respectively. The charge transfer resistance values were obtained from the diameter of the semicircles of the Nyquist plots. The inhibition efficiency of the inhibitor has been found out from the charge transfer resistance values using the following equation:

$$\eta\% = \frac{R_{\text{ct}}' - R_{\text{ct}}^0}{R_{\text{ct}}'} \times 100 \quad (6)$$

Where,  $R_{\text{ct}}^0$  and  $R_{\text{ct}}'$  are the charge transfer resistance in absence and in presence of inhibitor, respectively. All electrochemical measurements were done in unstirred and non-de-aerated solutions.

## FTIR

FTIR spectra were recorded in a Thermo Nicolet-5700 FTIR spectrophotometer (USA). The mild steel specimens of size  $2.5 \times 2.0 \times 0.025 \text{ cm}$  were prepared as described above. These specimens were immersed for  $3 \text{ h}$  in  $100 \text{ mL}$  of  $1 \text{ M HCl}$  solution containing  $400 \text{ ppm}$  of inhibitor and were then dried. In order to prevent damage of the protective film or layer of the mild steel surfaces, the FTIR reflectance accessory was applied to study the mild steel surfaces.

## Results and discussion

### Weight loss studies

#### Effect of Inhibitor concentration

Figure 1a represents the effect of inhibitor concentration on inhibition efficiency in HCl. The extract showed maximum inhibition efficiency of  $98\%$  in HCl and at an optimum concentration of  $400 \text{ ppm}$ . Further increase in extract concentration did not cause any significant change in the

performance of the extract. The values of percentage inhibition efficiency ( $\eta\%$ ) and corrosion rate ( $C_R$ ) obtained from weight loss method at different concentrations of Karanj (*P. pinnata*) seed extract at  $308 \text{ K}$  are summarized in Table 1.

#### Effect of immersion time

In order to assess the stability of inhibitive behavior of seed extract on a time scale, weight loss measurements were performed in  $1 \text{ M HCl}$  in absence and presence of seed extract at  $400 \text{ ppm}$  concentration for  $2\text{--}8 \text{ h}$  immersion time at temperature  $308 \text{ K}$ . Inhibition efficiencies were plotted against immersion time as seen from Fig. 1b. This figure shows that inhibition efficiency of the extract was increased with increasing immersion time from  $2$  to  $8 \text{ h}$  (give values). The increase in inhibition efficiency up to  $8 \text{ h}$  reflects the strong adsorption of constituents present in the extract on the mild steel surface, resulting in a more protective layer formed at mild steel/hydrochloric acid solution interface. Thus, Karanj (*P. pinnata*) seed extract effectively inhibit the mild steel corrosion in  $1 \text{ M}$  hydrochloric acid solutions.

#### Effect of acid concentration

The variation of inhibition efficiency with increase in acid concentration from  $0.5$  to  $2 \text{ M}$  is shown in Fig. 1c. From this figure, it can be seen that inhibition efficiency decreases from  $96\%$  to  $77\%$  with increase in HCl concentration from  $0.5$  to  $2 \text{ M}$ . This decrease in efficiency ( $\eta\%$ ) can be attributed to increased aggressiveness of solutions with increase in acid concentration.

#### Effect of temperature

To evaluate the stability of adsorbed layer/film of inhibitor on mild steel surface as well as activation parameters of the corrosion process of steel in acidic medium, weight loss measurements were carried out in the range of temperature  $308\text{--}338 \text{ K}$  in the absence and presence of extract at optimum concentration during  $3 \text{ h}$  immersion time. Results thus obtained are shown in Fig. 1d. It is evident from Fig. 1d that inhibition efficiency decreases with increasing temperature. This is due to increased rate of dissolution process of mild steel and partial desorption of the inhibitor from the metal surface with temperature [23].

The log of corrosion rate is a linear function of temperature (Arrhenius equation) [24–26]:

$$\log(C_R) = \frac{-E_a}{2.303RT} + A \quad (7)$$

where,  $E_a$  is the apparent effective activation energy,  $R$  is the general gas constant, and  $A$  is Arrhenius pre-exponential factor. A plot of log of corrosion rate obtained by weight

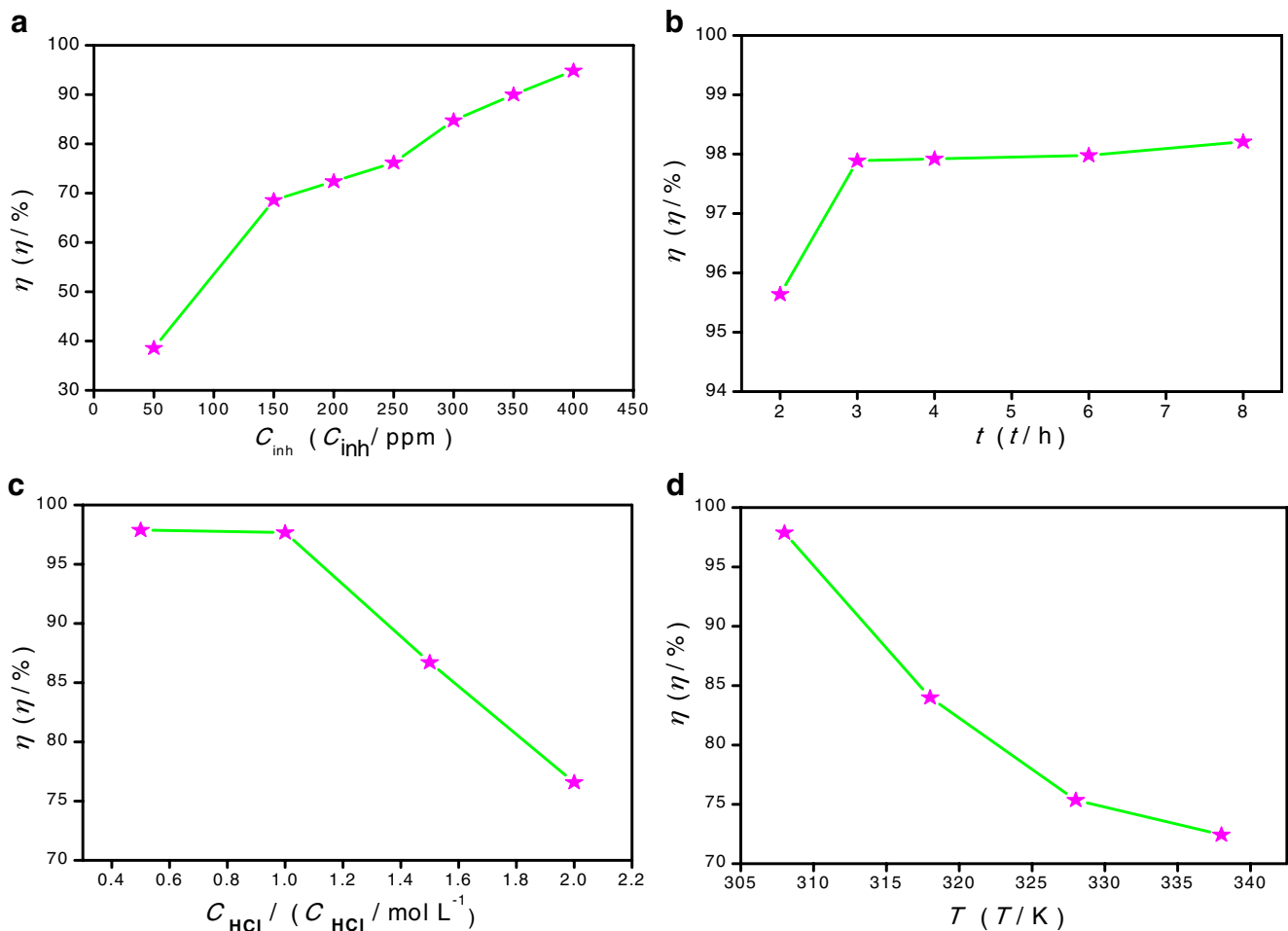


**Fig. 1** Variation of inhibition efficiency of Karanj (*P. pinnata*) extracts in 1 M HCl with **a** extract concentration, **b** immersion time, **c** acid concentration, and **d** temperature of the solution

loss measurement versus  $1/T$  gave a straight line as shown in Fig. 2a with a slope of  $-E_a/2.303 R$ . The values of activation energy are listed in Table 2. The data show that the activation energy ( $E_a$ ) of the corrosion in mild steel in 1 M HCl solution in the presence of extract is higher than that in the free acid solution. The increase in the apparent activation energy for mild steel dissolution in inhibited solution may be interpreted as physical adsorption that occurs in the first stage [27]. Szauer and Brand explained

[28] that the increase in activation energy can be attributed to an appreciable decrease in the adsorption of the inhibitor on the mild steel surface with increase in temperature.

An alternative formulation of Arrhenius equation is [29]:

$$C_R = \frac{RT}{Nh} \exp\left(\frac{\Delta S^*}{R}\right) \exp\left(\frac{-\Delta H^*}{RT}\right) \quad (8)$$

where,  $h$  is plank's constant,  $N$  is Avogadro's number,  $\Delta S^*$  the entropy of activation, and  $\Delta H^*$  the enthalpy of

**Table 1** Corrosion parameters for mild steel in aqueous solution of 1 M HCl in presence and absence of different concentrations of Karanj (*Pongamia pinnata*) seed extract from weight loss measurements at 308 K for 3 h

Inhibitor concentration (ppm)	Weight loss ( $mgcm^{-2}$ )	$\eta$ (%)	$C_R$ ( $mmyear^{-1}$ )
1 M HCl	20.9	–	77.9
50	13.0	39	48.2
150	6.6	69	24.5
200	5.8	72	21.5
250	2.5	88	9.3
300	1.7	92	6.3
350	1.1	95	4.0
400	0.5	98	1.8

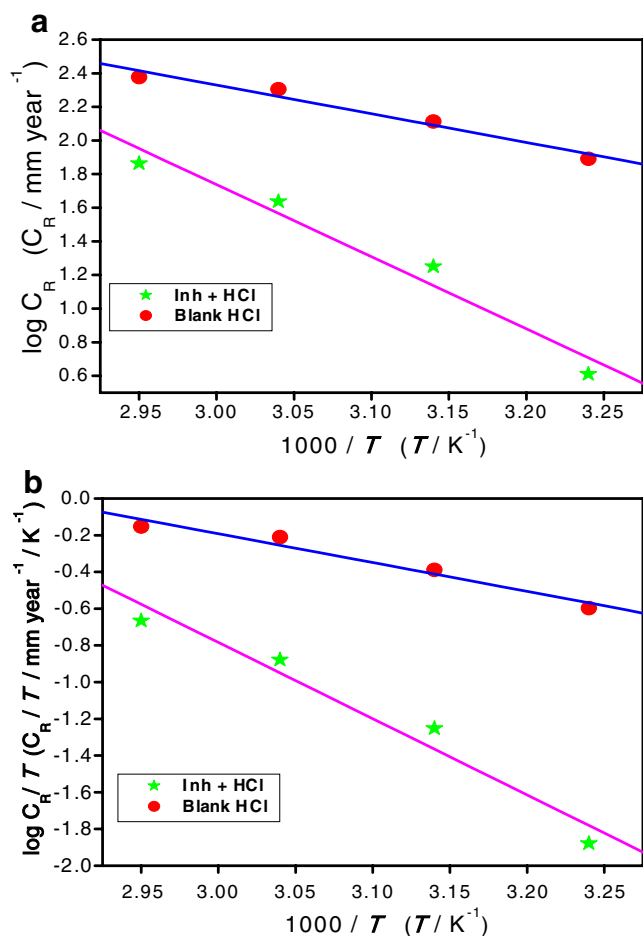


**Fig. 2** Adsorption isotherm plots for **a**  $\log C_R$  ( $C_R/\text{mmyear}^{-1}$ ) vs.  $1,000/T$  ( $T/\text{K}^{-1}$ ) and **(b)**  $\log C_R/T$  ( $C_R/T \text{ mmyear}^{-1}/\text{K}^{-1}$ ) vs.  $1,000/T$  ( $T/\text{K}^{-1}$ )

activation. A plot of  $\log C_R/T$  versus  $1/T$  gave a straight line (Fig. 2b) with a slope equal to  $-\Delta H^*/2.303 R$  and an intercept of  $\log R/Nh + \Delta S^*/2.303 R$ , from which the values of  $\Delta S^*$  and  $\Delta H^*$  were calculated and listed in Table 2. The positive signs of enthalpies ( $\Delta H^*$ ) reflect the endothermic nature of dissolution process. This suggests that mild steel dissolution requires more energy in 1 M HCl in the presence of seed extract. The shift towards positive value of entropies ( $\Delta S^*$ ) imply that the activated complex in the rate determining step represents dissociation rather than association, meaning that disordering increases on going from reactants to the activated complex [30].

**Table 2** The values of activation parameters  $E_a$ ,  $\Delta H^*_a$ ,  $\Delta S^*_a$  for mild steel in 1 M HCl in the absence and presence of optimum concentrations of Karanj (*Pongamia pinnata*) seed extract

Inhibitor conc. (ppm)	$E_a$ ( $\text{kJmol}^{-1}$ )	$\Delta H^*_a$ ( $\text{kJmol}^{-1}$ )	$\Delta S^*_a$ ( $\text{J K}^{-1}\text{mol}^{-1}$ )	$K_{\text{ads}}$ ( $\text{M}^{-1}$ )	$\Delta G^\circ_{\text{ads}}$ ( $\text{kJmol}^{-1}$ )
1 M HCl	28	22	-136	–	–
400 ppm	82	80	26	41,256	37

EIS measurement

Impedance spectra for mild steel in 1 M HCl in absence and presence of different concentrations of Karanj (*P. pinnata*) seed extract are shown in the form of Nyquist plots (Fig. 3a), Bode-modulus plots (Fig. 3b) and Bode plots in the Theta-frequency format (Fig. 3c). It can be seen from Fig. 3 that diameter of the semicircular capacitive loop (Fig. 3a), and phase angle (Fig. 3c) increased with increasing concentration of seed extract, and impedance of the double layer (Fig. 3b) decreased with extract concentration. Nyquist plots consist of a “depressed” semicircle with one capacitive loop and depressed semicircle has a center under the real axis. Such behavior is characteristic for solid electrodes and often referred to as frequency dispersion and has been attributed to roughness and other inhomogeneities of solid surface [31, 32]. The Nyquist plots show a depressed capacitive loop in the high-frequency (HF) range and an inductive loop in the lower-frequency (LF) range. The HF capacitive loop can be attributed to the charge transfer reaction and time constant of the electric double layer and to the surface inhomogeneity of structural or interfacial origin, such as those found in adsorption processes [33]. The LF inductive loop may be attributed to the relaxation process obtained by adsorption species like  $\text{Cl}^-_{\text{ads}}$  and  $\text{H}^+_{\text{ads}}$  on the electrode surface and might also be attributed to the re-dissolution of the passivates surface at low frequencies. The fact that this semicircle cannot be observed after the addition of higher concentration supports our view [34, 35].

The impedance spectra for Nyquist plots were analyzed by fitting to the equivalent circuit model (Fig. 4) which was used elsewhere to describe iron/acid interface [36]. This equivalent circuit consists of CPE  $Q$  ( $n=1$ ,  $Q=C_{\text{dl}}$ ) in parallel to the series resistors  $R_{\text{ct}}$  and an inductor ( $L$ ). Further,  $R_s$  is the solution resistance. The impedance of CPE values were calculated using the equation [37]:

$$Z_{\text{CPE}} = Q^{-1}(j\omega)^{-n} \tag{9}$$

where  $Q$  is the CPE constant,  $j$  is the imaginary unit,  $\omega$  is the angular frequency ( $\omega=2\pi f$ , the frequency in Hz), and  $n$  is the CPE exponent which can be used as a gauge of the heterogeneity and gives details about the degree of surface inhomogeneity (roughness). Depending on the value of  $n$ , CPE can represent resistance ( $n=0$ ,  $Q=1/R$ ), capacitance

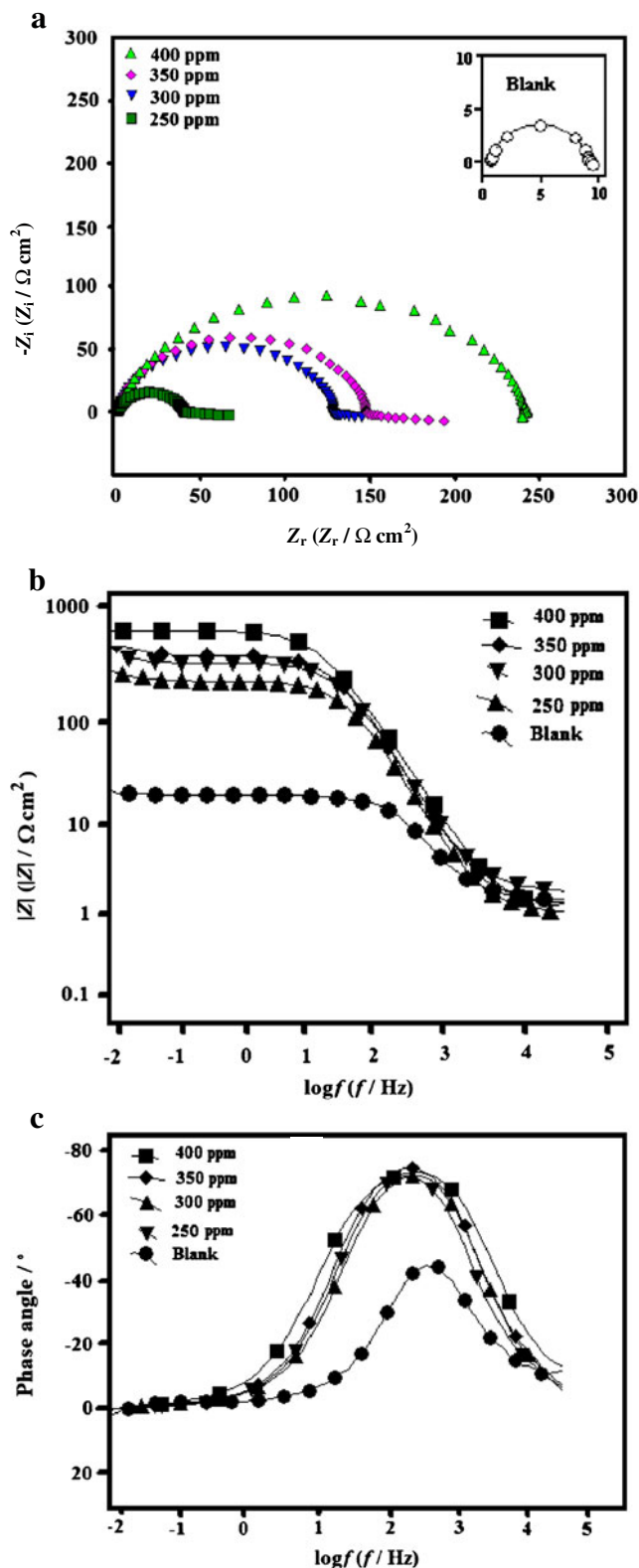


**Fig. 3** a Nyquist plots, b Bode-modulus plots, and c Bode-phase angle plots in absence and presence of different concentrations of extract in 1 M HCl

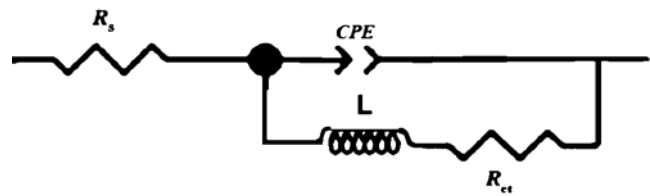


**Fig. 4** Electrochemical equivalent circuit used to fit the impedance spectra

( $n=1$ ,  $Q=C$ ), inductance ( $n=-1$ ,  $Q=1/L$ ) or Warburg element ( $n=0.5$ ). When  $n=1$ , this is the same equation as that for the impedance of a capacitor, where  $Q=C_{dl}$ . In fact, when  $n$  is close to 1, the CPE resembles a capacitor, but the phase angle is not  $90^\circ$ . It is constant and somewhat less than  $90^\circ$  at all frequencies.

In spite of the mentioned fact, the term, double-layer capacitance, is still often used in the evaluation of AC impedance results to characterize the double layer believed to be formed at the metal/solution interface of systems displaying non-ideal capacitive behavior. For providing simple comparison between the capacitive behaviors of different corrosion systems, the values of  $Q$  were converted to  $C_{dl}$ .

$$C_{dl} = Q(\omega_{max})^{n-1} \quad (10)$$

here,  $\omega_{max}$  represents the frequency at which the imaginary component reaches a maximum. It is the frequency at the top of the depressed semicircle, and it is also the frequency at which the real part ( $Z_r$ ) is midway between the low and high frequency x-axis intercepts.

The impedance parameters such as solution resistance ( $R_s$ ), charge transfer resistance ( $R_{ct}$ ),  $Q$ ,  $n$ , derived double-layer capacitance ( $C_{dl}$ ), and inhibition efficiency ( $\eta$  %) are listed in Table 3. The values of  $\eta$  % are calculated using the following equation:

$$\eta(\%) = \frac{R_{ct,i} - R_{ct,0}}{R_{ct,i}} \times 100 \quad (11)$$

where,  $R_{ct,i}$  and  $R_{ct,0}$  are charge transfer resistances in presence and absence of inhibitor, respectively. It is clear from Table 3 that by increasing the inhibitor concentration, the  $C_{dl}$  values tend to decrease and the inhibition efficiency increases. The decrease in  $C_{dl}$  values can be attributed to a decrease in local dielectric constant and/or an increase in the thickness of the electrical double layer, suggesting that Karanj (*P. pinnata*) seed extract act by adsorption at the mild steel/solution interface [38]. On the other hand, the values of  $C_{dl}$  decreased with an increase in the extract concentration. This situation was the result of an increase in the surface coverage by the inhibitor, which led to an increase in the inhibition efficiency. The values of the phase shift indicate that the  $C_{dl}$  values are in reasonable confidence limit. Also any significant change in

**Table 3** Electrochemical impedance parameters for mild steel in 1 M HCl in absence and presence of different concentrations of Karanj (*Pongamia pinnata*) seed extract

Acid solution	Inhibitor (ppm)	$R_s$ ( $\Omega$ cm <sup>2</sup> )	$R_{ct}$ ( $\Omega$ cm <sup>2</sup> )	$L$ ( $10^{-3}$ H)	$Q$ ( $10^{-6}\Omega^{-1}$ s <sup>n</sup> cm <sup>-2</sup> )	Number	$C_{dl}$ ( $\mu$ Fcm <sup>-2</sup> )	$\eta$ (%)
1 M HCl	0	1.2	9±0.04	5	1,120	0.827	301	–
	250	1.2	41±0.2	13	181	0.842	65	79
	300	1.5	130±0.7	53	93	0.877	49	93
	350	1.2	152±0.8	68	91	0.880	48	94
	400	1.0	241±1.0	93	86	0.853	44	96

the values of the phase shift,  $n$ , was not observed in the absence and in the presence of Karanj (*P. pinnata*). To predict the dissolution mechanism, the value of  $n$  can be used as an indicator [39]. The values of  $n$ , ranging between 0.827 and 0.880, indicate that the charge transfer process controls the dissolution mechanism of mild steel in 1 M HCl solution in the absence and in the presence of seed extract. The thickness of the protective layer,  $\delta_{org}$ , was related to  $C_{dl}$  by the following equation [40]:

$$\delta_{org} = \frac{\epsilon_0 \epsilon_r}{C_{dl}} \tag{12}$$

where,  $\epsilon_0$  is the dielectric constant and  $\epsilon_r$  is the relative dielectric constant. This decrease in the  $C_{dl}$ , which can result from a decrease in local dielectric constant and/or an increase in the thickness of the electrical double layer, suggested that Karanj (*P. pinnata*) seed extract function by adsorption at the metal/solution interface. Thus, the change in  $C_{dl}$  values was caused by the gradual replacement of water molecules by the adsorption of the organic molecules on the metal surface, decreasing the extent of metal dissolution [41].

It is apparent from Nyquist plots that the impedance response of mild steel in inhibited HCl solution has significantly changed after the addition of Karanj (*P. pinnata*) seed extract in acid solution and that the impedance of inhibited substrate increases with increasing conc. of inhibitor. The Nyquist plots showed that on increasing Karanj (*P. pinnata*) concentration, increases charge transfer resistance and decreases double layer capacitance. From Table 3, it is clear that the greatest effect was observed at 400 ppm of Karanj (*P. pinnata*) extract which gives  $R_{ct}$  value of 240  $\Omega$ cm<sup>2</sup> in 1 M HCl, respectively. Inhibition efficiency is found to increase with inhibitor concentration in the acid. The data obtained from EIS are in good agreement with those obtained from weight loss method.

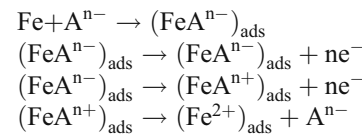
**Polarization measurements**

Polarization curves for mild steel at various concentration of Karanj (*P. pinnata*) seed extract in aerated solutions are shown in Fig. 5. The extrapolation of Tafel straight line

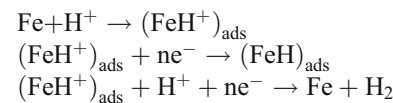
allows the calculation of the corrosion current density ( $I_{corr}$ ). The values of  $I_{corr}$ , the corrosion potential ( $E_{corr}$ ), cathodic and anodic Tafel slopes ( $b_c$ ,  $b_a$ ), and inhibition efficiency ( $\eta$  %) are given in Table 4. The ( $\eta$  %) is calculated using the following equation:

$$\eta\% = \left( \frac{I_{corr}^0 - I_{corr}^i}{I_{corr}^0} \right) \times 100 \tag{13}$$

Where,  $I_{corr}^0$  and  $I_{corr}^i$  are the corrosion current density values without and with inhibitor, respectively. Some of the authors proposed the following mechanism for the corrosion of iron and steel in acid solution [42–44]:



The cathodic hydrogen evolution



The change in  $b_a$  and  $b_c$  values as shown in Table 4 indicates that adsorption of Karanj (*P. pinnata*) seed extract modify the mechanism of anodic dissolution as well as cathodic hydrogen evolution. From Fig. 5, it is clear that

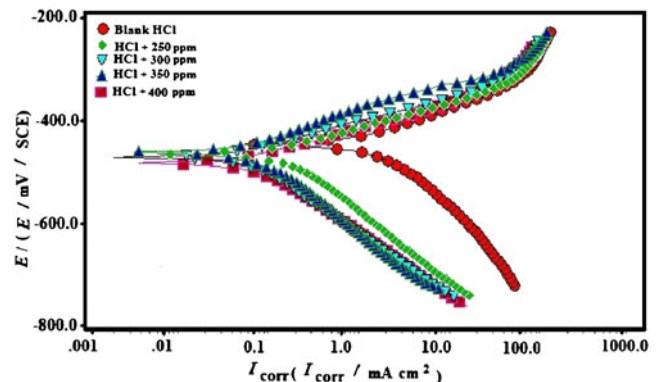
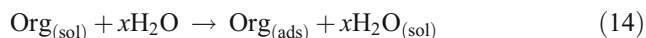


**Fig. 5** Polarization curves in the absence and presence of different concentrations of extract in 1 M HCl

both the cathodic and anodic reactions are inhibited, and the inhibition increases as the inhibitor conc. increases in acid media, but the cathode is more polarized. From Table 4, it is clear that there was no definite trend in the shift of  $E_{\text{corr}}$  values, in the presence of various conc. of Karanj (*P. pinnata*) seed extract in 1 M HCl solution. This result indicated that Karanj (*P. pinnata*) seed extract can be classified as mixed type of inhibitor in 1 M HCl solution.

#### Adsorption isotherm and free energy of adsorption

The adsorption of an organic adsorbate on to metal–solution interface can be represented by a substitutional adsorption process between the organic molecules in the aqueous solution phase ( $\text{Org}_{(\text{sol})}$ ) and the water molecules on the metallic surface ( $\text{H}_2\text{O}_{(\text{ads})}$ ) [45].



where,  $x$  is the size ratio representing the number of water molecules replaced by one molecule of organic adsorbate. Basic information on the interaction between the inhibitor and the mild steel surface can be provided by the adsorption isotherm. For this purpose, the values of surface coverage ( $\theta$ ) at different concentrations ( $C_{\text{inh}}$ ) of Karanj (*P. pinnata*) seed extract in acid media in the temperature range (308–338 K) have been used to explain the best isotherm to determine the adsorption process. The values of  $\theta$  can be easily determined from the ratio  $((\eta\%)/100)$ , where ( $\eta\%$ ) was obtained from weight loss measurements. Attempts were made to fit these  $\theta$  values to various isotherm including Frumkin, Langmuir, Temkin. According to these isotherms,  $\theta$  is related to the inhibitor concentration,  $C_{\text{inh}}$ :

$$\theta = \frac{bC_{\text{inh}}}{1+bC_{\text{inh}}} \quad (\text{Langmuir isotherm}) \quad (15)$$

$$\exp(-2a\theta) = K_{\text{ads}}C_{\text{inh}} \quad (\text{Temkin isotherm}) \quad (16)$$

where,  $b$  designates the adsorption coefficient in Eq. (15),  $a$  the molecular interaction parameter,  $K_{\text{ads}}$  is the equilibrium

constant of the adsorption process in Eq. 16. The best fit was obtained with Langmuir isotherm as shown in Fig. 6. The value of regression coefficients ( $R^2=0.994$ ) confirms the validity of this approach. The equilibrium constant of adsorption ( $K_{\text{ads}}$ ) is related to the standard free energy of adsorption ( $\Delta G_{\text{ads}}^\circ$ ) by the relation [46]:

$$K_{\text{ads}} = \left(\frac{1}{55.5}\right) \exp\left(-\frac{\Delta G_{\text{ads}}^\circ}{RT}\right) \quad (17)$$

where  $R$  is the universal gas constant,  $T$  the absolute temperature, and the value of 55.5 is the concentration of water in  $\text{mol l}^{-1}$  in the solution [47].

The values of  $K_{\text{ads}}$  and  $\Delta G_{\text{ads}}^\circ$  calculated from Eq. 17 are listed in Table 2. The high value of  $K_{\text{ads}}$  for studied extract indicates stronger adsorption on the mild steel surface in 1 M HCl solution. The strong interaction of inhibitor with mild steel surface can be attributed to the presence of  $O$ -atoms and  $\pi$ -electrons in the inhibitor molecules. Lagrenee et al. [48] have reported that the higher  $K_{\text{ads}}$  value (approximately  $>100 \text{ M}^{-1}$ ), the stronger and more stable adsorbed layer is formed which results in the higher inhibition efficiency.

The negative value of  $\Delta G_{\text{ads}}^\circ$  for the adsorption of extract's constituents on the mild steel surface suggests the spontaneity of the adsorption process and the stability of the adsorbed layer on the mild steel surface. Generally,  $\Delta G_{\text{ads}}^\circ$  values of  $-20 \text{ kJ mol}^{-1}$  or higher are associated with an electrostatic interaction between charged molecules and charged metal surface, physisorption; those of  $-40 \text{ kJ mol}^{-1}$  or lower involve charge sharing or transfer from the inhibitor molecules to the metal surface to form a coordinate covalent bond, chemisorption [49]. In present case,  $\Delta G_{\text{ads}}^\circ$  was  $-37 \text{ kJ mol}^{-1}$  at 308 K indicating the adsorption of investigated seed extract on mild steel surface is neither typical physisorption nor typical chemisorption, but it is complex mixed type that is the adsorption of inhibitor molecules on the mild steel surface in present study involves both physisorption and chemisorption and electrostatic interaction (physisorption) is predominant.

**Table 4** Potentiodynamic polarization parameters for mild steel without and with different concentrations of Karanj (*Pongamia pinnata*) seed extract in 1 M HCl

Conc. of inhibitor (ppm)	Tafel data					Linear polarization data	
	$E_{\text{corr}}$ (mV vs. SCE)	$I_{\text{corr}}$ ( $\mu\text{A cm}^{-2}$ )	$\beta_a$ (mV dec $^{-1}$ )	$\beta_c$ (mV dec $^{-1}$ )	$\eta$ (%)	$R_p$ ( $\Omega \text{ cm}^2$ )	$\eta$ (%)
1 M HCl	-446	1,540	90	121	–	10	–
250	-465	142	57	111	91	71	86
300	-461	84	89	136	94	160	94
350	-482	77	65	118	95	184	95
400	-471	49	55	76	97	246	96



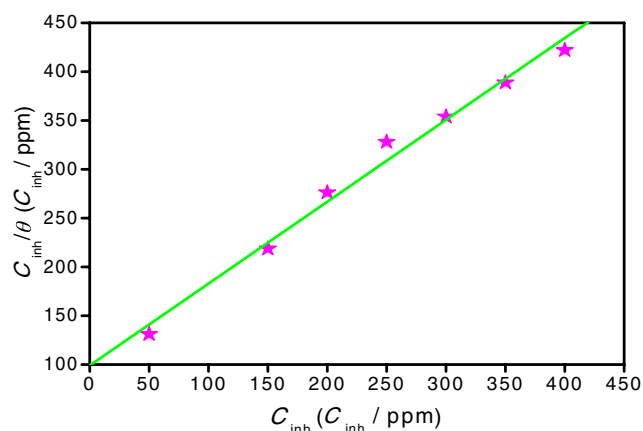


**Fig. 6** Langmuir adsorption isotherm plot for the adsorption of extract in 1 M HCl on the surface of mild steel

Further, this assumption is supported by data obtained from temperature dependence of inhibition process (Fig. 1d). Thus, adsorption of investigated seed extract on the mild steel surface in 1 M HCl is complex in nature. Similar assumptions were reported in literature [50].

#### FTIR analysis

It has been established that FTIR spectrophotometer is a powerful instrument that can be used to determine the type of bonding for organic inhibitors adsorbed on the metal surface. In present study, reflectance FTIR spectra were used to support the fact that corrosion inhibition of mild steel in acid media is due to the adsorption of inhibitor molecules on the mild steel surface. The prominent peaks are given in Table 5. From data in Table 5, it can be established that inhibition of corrosion of mild steel in 1 M HCl solution by Karanj (*P. pinnata*) seed extract was due to the adsorption of extract's constituents on the mild steel surface.

#### Mechanism of inhibition

The transition of metal/solution interface from a state of active dissolution to the passive state is attributed to the adsorption of the inhibitor molecules at the metal/solution interface, forming a protective film. The rate of adsorption is usually rapid; hence, the reactive metal surface is shielded from the aggressive environment [51].

Adsorption process can occur through the replacement of solvent molecules from metal surface by ions and molecules accumulated in the vicinity of metal/solution interface. Ions can accumulate at the metal/solution interface in excess of those required to balance the charge on the metal at the operating potential. These ions replace solvent

molecules from the metal surface and their centers reside at the inner Helmholtz plane. This phenomenon is termed specific adsorption, contact adsorption. The anions are adsorbed when the metal surface has an excess positive charge in an amount greater than that required to balance the charge corresponding to the applied potential. Aromatic compounds (which contain the benzene ring) undergo particularly strong adsorption on many electrode surfaces. The bonding can occur between metal surface atoms and the aromatic ring of the adsorbate molecules or ligands substituent groups. The exact nature of the interactions between a metal surface and an aromatic molecule depends on the relative coordinating strength towards the given metal of the particular groups present [52].

The main constituents of extract of Karanj (*P. pinnata*) seed are Karanjin (3-methoxy-2-phenyl-4H-furo [2,3-*h*]chromen-4-one), Pongapin (2-(benzo[*d*][1,3]dioxol-5-yl)-3-methoxy-4*H*-furo[2,3-*h*]chromen-4-one), Kanjone (6-methoxy-2-phenyl-4H-furo[2,3-*h*]chromen-4-one), and Pongaglabrone (2-(benzo[*d*][1,3]dioxol-5-yl)-4*H*-furo[2,3-*h*]chromen-4-one) whose structures are given in Fig. 7 [53, 54]. The high performance of Karanj (*P. pinnata*) extract could also be due to large size of constituent's molecule which covers wide areas on the metal surface and thus retarding the corrosion [55].

It is not possible to consider a single adsorption mode between inhibitor and metal surface because of the complex nature of adsorption and inhibition of a given inhibitor. The adsorption of main constituents of seed extract can be attributed to the presence of *O*-atoms,  $\pi$ - electrons, and aromatic/heterocyclic rings. Presence of methoxy group also enhances the inhibition efficiency. Therefore, the possible reaction centers are unshared electron pair of hetero-atoms and  $\pi$ -electrons of aromatic/heterocyclic ring. In aqueous acidic solutions, main constituents exist either as neutral molecules or as protonated molecules (cations). The inhibitors may adsorb on the metal/acid solution interface by one and/or more of the following ways: (1)

**Table 5** Prominent peaks obtained from reflectance FTIR spectroscopy

Frequency (cm <sup>-1</sup> )	Band assignment
679	C–F stretching
1,082	C–O stretching
1,226	C–N stretching
1,373	C=C (aromatic)
1,528	C=C (aromatic)
1,725	C=O stretching
2,883	C–H stretching
3,268	N–H stretching

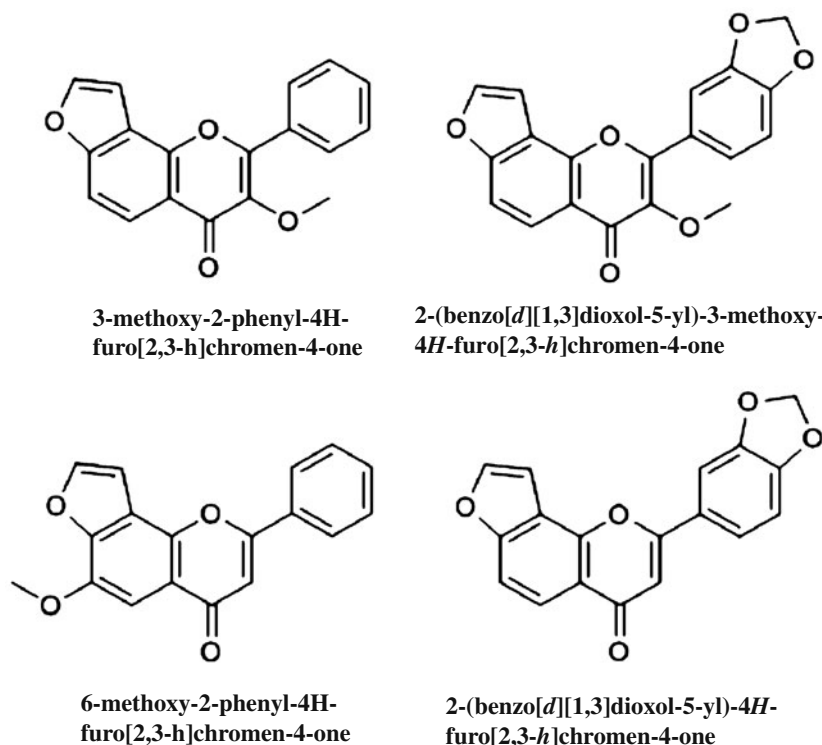


**Fig. 7** Structure of main constituents of Karanj (*P. pinnata*) seed extract

electrostatic interaction of protonated molecules with already adsorbed chloride ions, (2) donor-acceptor interactions between the  $\pi$ -electrons of aromatic ring and vacant d orbital of surface iron atoms, (3) interaction between unshared electron pairs of hetero atoms and vacant d-orbital of iron surface atoms.

Generally, two modes of adsorption are considered on the metal surface in acid media. In one mode, the neutral molecules may be adsorbed on the surface of mild steel through the chemisorption mechanism, involving the displacement of water molecules from the mild steel surface and the sharing electrons between the hetero atoms and iron. The inhibitor molecules can also adsorb on the mild steel surface on the basis of donor-acceptor interactions between  $\pi$ -electrons of the aromatic/heterocyclic ring and vacant d-orbitals of surface iron atoms. In second mode, since it is well known that the steel surface bears positive charge in acid solution [56], it is difficult for the protonated molecules to approach the positively charged mild steel surface ( $\text{H}_3\text{O}^+$ /metal interface) due to the electrostatic repulsion. Since chloride ions have a smaller degree of hydration, they could bring excess negative charges in the vicinity of the interface and favor more adsorption of the positively charged inhibitor molecules, the protonated inhibitors adsorb through electrostatic interactions between the positively charged molecules and the negatively charged metal surface. Thus, there is a synergism between

adsorbed  $\text{Cl}^-$  ions and protonated inhibitors. Thus, inhibition of mild steel corrosion in 1 M HCl is due to the adsorption of extract constituents on the mild steel surface. This assumption could be further confirmed by the reflectance FTIR analysis of mild steel surface.

## Conclusions

1. Karanj (*P. pinnata*) seed extract is a good inhibitor for mild steel corrosion in 1 M HCl solution. Inhibition efficiency increases with increasing seed extract concentration, and  $\eta$  % values obtained from different methods employed are in reasonable agreement.
2. The adsorption of Karanj (*P. pinnata*) seed extract on mild steel surface obeyed Langmuir adsorption isotherm with free energy of adsorption  $37 \text{ kJmol}^{-1}$ , and adsorption is neither typical physisorption nor typical chemisorption but complex in nature.
3. Polarization curves measurements indicate that Karanj (*P. pinnata*) seed extract acted as mixed type inhibitor.
4. The increasing value of CPE exponent, i.e., the phase shift ( $n$ ) with increasing inhibitor concentration indicated that surface roughness decreased with increasing inhibitor concentration.
5. The reflectance FTIR analysis showed that the inhibition of mild steel corrosion occurred due to the

formation of a protective film on the metal surface through adsorption of constituents of Karanj (*P. pinnata*) seed extract.

## References

- Ashassi-Sorkhabi H, Seifzadeh D, Hosseini MG (2008) Corros Sci 50:3363–3370
- Satapathy AK, Gunasekaran G, Sahoo SC, Kumar A, Rodrigues PV (2009) Corros Sci 51:2848–2856
- Abdel-Gaber AM, Abd-El-Nabey BA, Saadawy M (2009) Corros Sci 51:1038–1042
- Raja PB, Sethuraman MG (2008) Mater Lett 62:113–116
- Noor EA (2008) J Eng Appl Sci 3:23–30
- Buchweishaija J, Mhinzi GS (2008) Port Electrochim Acta 26:257–265
- Oguzie EE (2008) Corros Sci 50:2993–2998
- Okafor PC, Ikpi ME, Uwaha IE, Ebenso EE, Ekpe UJ, Umoren SA (2008) Corros Sci 50:2310–2317
- Valek L, Martinez S (2007) Mater Lett 61:148–151
- Okafor PC, Ikpi ME, Uwaha IE, Ebenso EE, Ekpe UJ, Umoren SA (2008) Corros Sci 50:2310–2317
- Noor EA (2009) J Appl Electrochem 39:1465–1475
- De Souza FS, Spinelli A (2009) Corros Sci 51:642–649
- Raja PB, Sethuraman MG (2008) Mater Lett 62:1602–1604
- El-Etre AY (2003) Corros Sci 45:2485–2495
- Badiaea AM, Mohana KN (2009) J Mater Eng Perform 18:1264–1271
- Chauhan LR, Gunasekaran G (2007) Corros Sci 49:1143–1161
- El-Etre AY, Abdallah M, El-Tantawy ZE (2005) Corros Sci 47:385–395
- Orubite KO, Oforka NC (2004) Mater Lett 58:1768–1772
- Evic Grassino AN, Grabaric Z, Pezzani A, Fasanaro G, Voi AL (2009) Food Chem Toxicol 47:1556–1561
- Torres-Acosta AA (2007) J Appl Electrochem 37:835–841
- Quraishi MA, Singh A, Singh VK, Yadav DK, Singh AK (2010) Mater Chem Phys 122:114–122
- Quraishi MA, Yadav DK, Ahamad I (2009) Open Corrosion J 2:56–60
- Schorr M, Yahalom J (1972) Corros Sci 12:867–868
- Quraishi MA, Khan S (2005) Indian J Chem Tech 12:576–581
- Breslin CB, Carrol WM (1993) Corros Sci 34:327–341
- Khedr MGA, Lashien MS (1992) Corros Sci 33:137–151
- Larabi L, Benali O, Harek Y (2007) Mater Lett 61:3287–3291
- Szauer T, Brandt A (1981) Electrochim Acta 26:1253–1256
- Bockris JOM, Reddy AKN (1977) Modern electrochemistry. Plenum, New York
- Prabhu RA, Shanbhag AV, Venkatesha TV (2007) J Appl Electrochem 37:491–497
- Elayyachy M, Idrissi A, Hammouti B (2006) Corros Sci 48:2470–2479
- Martinez S, Metikos-Hukovic M (2003) J Appl Electrochem 33:1137–1142
- Goncalves RS, Azambuja DS, Serpa Lucho AM (2002) Corros Sci 44:467–479
- Amin MA, Abd El-Rehim SS, El-Sherbini EEF, Bayyomi RS, Amin MA, Abd El-Rehim SS, El-Sherbini EEF, Bayyomi RS (2007) Electrochim Acta 52:3588–3600
- Kedam M, Mattos OR, Takenouti H (1981) J Electrochem Soc 128:257–266
- Mansfeld F (1981) Corrosion 36:301–307
- Shukla J, Pitre KS (2002) Corros Rev 20:217–229
- Yurt A, Bereket G, Kivrak A, Balaban A, Erk B (2005) J Appl Electrochem 35:1025–1032
- Hermas AA, Morad MS, Wahdan MH (2004) J Appl Electrochem 34:95–102
- Bentiss F, Mehdi B, Mernari B, Traisnel M, Vezin H (2002) Corrosion 58:399–407
- Anand RR, Hurd RM, Hackerman N (1965) J Electrochem Soc 112:138–144
- Morad MS, El-Dean AMK (2006) Corros Sci 48:3398–3412
- Tebbji K, Hammouti B, Oudda H, Ramdani A, Benkadour M (2005) Appl Surf Sci 252:1378–1385
- Yurt A, Balaban A, Ustun Kandemir S, Bereket G, Erk B (2004) Mater Chem Phys 85:420–426
- Gomma GK, Wahdan MH (1994) Mater Chem Phys 39:142–148
- Kaminski M, Szklarska-Smialowska Z (1973) Corros Sci 13:557–565
- Olivares O, Likhanova NV, Gomez B, Navarrete J, Llanos-Serrano ME, Arce E, Hallen JM (2006) Appl Surf Sci 252:2894–2909
- Lagrenée M, Mernari B, Bouanis M, Traisnel M, Bentiss F (2002) Corros Sci 44:573–588
- Hosseini M, Mertens SFL, Arshadi MR (2003) Corros Sci 45:1473–1489
- Li W-H, He Q, Zhang S-T, Pei C-L, Hou B-R (2008) J Appl Electrochem 38:289–292
- Chao CY, Lin LF, Macdonald DD (1981) J Electrochem Soc 128:1187–1194
- Ritchie IM, Bailey S, Woods R (1999) Adv Colloid Interface Sci 80:183–231
- Khanna RN, Seshadri TR (1964) Curr Sci 33:644–645
- Vohra S (2008) Ph.D. Thesis, Jamia Millia Islamia, New Delhi, India
- Trabenelli G, Mansfeld F (1987) Corrosion mechanisms. Marcel Dekker, New York, p 109
- Mu GN, Zhao TP, Liu M, Gu T (1996) Corrosion 52:853–856